DOI: 10.1002/ejic.200701032

Structural Diversity in Organotin Compounds Derived from Bulky Monoaryl Phosphates: Dimeric, Tetrameric, and Polymeric Tin Phosphate Complexes

Ramaswamy Murugavel,*[a] Swaminathan Shanmugan,[a] and Subramaniam Kuppuswamy[a]

Keywords: Organotin compounds / Polymers / Cluster compounds / Precursors / X-ray structures

Monoaryl phosphates with a bulky aryl substituent have been used to synthesize new organotin clusters and polymers. The equimolar reaction between 2,6-diisopropylphenylphosphate (dipp-H_2) and Me_2SnCl_2 in ethanol at 25 °C leads to the formation of $[Me_2Sn(\mu_3\text{-dipp})]_n$ (**1**), while the reaction of 2,6-dimethylphenylphosphate (dmpp-H_2) with Me_2SnCl_2 in either a 1:1 or 2:1 molar ratio proceeds to produce exclusively $[Me_2Sn(\mu\text{-dmpp-H})_2]_n{\cdot}nH_2O$ (**2**). Compounds **1** and **2** are 1D polymers with different architectures. In compound **1**, the tin atom is five-coordinate (trigonal bipyramidal). Each dipp ligand bridges three different tin atoms to form an infinite ladder-chain structure. In **2**, each six-coordinate (octahedral) tin atom is surrounded by four phosphate oxygen atoms originating from four different bridging dmpp-H ligands, thus forming a spirocyclic coordination polymeric chain. The use of nBu$_2$SnO as the diorganotin source in its reaction with dipp-H_2 leads to the isolation of dimeric $[n\text{Bu}_2\text{Sn}(\mu\text{-dipp-H})(\text{dipp-H})]_2$ (**4**), which contains a central $Sn_2O_4P_2$ unit. There are two chemically different half molecules of **4** in the asymmetric part of the unit cell and hence it actually exists as a 1:1 mixture of $[n\text{Bu}_2\text{Sn}(\mu\text{-dipp-H})(\text{dipp-H})]_2$ and $[n\text{Bu}_2\text{Sn}(\mu\text{-dipp})(\text{dipp-H}_2)]_2$ in the solid state. The reaction of the monoorgano tin precursor nBuSn(O)(OH)·xH_2O with dipp-H_2 takes place in acetone at room temperature to yield the tetrameric cluster **5**, which has different structures in the solution and in the solid state. ^{31}P NMR spectroscopy clearly suggests that **5** has the formula $[n\text{Bu}_4\text{Sn}_4(\mu\text{-O})_2(\mu\text{-dipp-H})_8]$ in solution. The single-crystal X-ray diffraction studies in the solid state, however, reveal that compound **5** exists as $[n\text{Bu}_4\text{Sn}_4(\mu\text{-OH})_2(\mu\text{-dipp-H})_6(\mu\text{-dipp})_2]$. The use of compounds **1**–**4** as possible precursors for the preparation of ceramic tin phosphate materials has been investigated. The thermolysis of **1** at 500 °C leads to the formation of quantitative amounts of $Sn_2P_2O_7$, while the thermolysis of **2**, **3**, and **4** under similar conditions results in the formation of SnP_2O_7.

Introduction

The use of ligands that contain more than one hydroxy group on a central main group element for the purpose of building multinuclear metal cages, clusters, and polymeric structures has gained greater momentum in the last two decades.[1] One of the main reasons for this flare-up of activity in this area is due to the realization that such cage structures could be transformed into super-structures that would resemble zeolite-like materials.[2] We have recently shown that 2,6-diisopropylphenylphosphate (dipp-H_2) is an ideal starting point for the preparation of both main group and transition-metal phosphate clusters that self-assemble through noncovalent interactions into zeolite-like materials.[3–5] For example, by using zinc as the representative example, it is possible to build hierarchical zinc–dipp structures in a systematic way by changing the coligands used.[3] Similarly large aluminophosphate clusters, often exceeding a molecular weight of 4000, can be isolated from 2,6-diisopropylphenylphosphate and a suitable aluminum precursor in nonaqueous medium.[4]

Fascinated by the variety of structures obtained for divalent transition metals such as zinc, manganese, and copper as well as the trivalent aluminum with dipp-H_2, we wished to unravel the types of structures that would be formed in the case of tetravalent tin. Interaction of organotin precursors with acidic hydrogen-containing compounds has been extensively studied in the 1980s and 1990s by Holmes et al., who unraveled several new structural types for tin.[6] After a dormant period in between, Chandrasekhar et al.[7] and others[8–10] showed in recent years that newer and more interesting tin aggregates and polymers could be synthesized by employing a variety of exotic and suitably designed carboxylic acids, phosphinic acids, sulfonic acids, and other acidic proton-containing main group ligands. Thus, while the interaction of both phosphinic[11–13] and phosphonic acids[11,14–17] with organotin precursors in the assembly of organostannoxane cages has been a subject of intense investigation for sometime now, the use of phosphate esters for this purpose has been limited to a few sporadic reports.[18] Owing to the important role played by bulky substituents in main group chemistry in recent times,

[a] Department of Chemistry, Indian Institute of Technology – Bombay,
Powai, Mumbai 400076, India
Fax: +22-2572-3480
E-mail: rmv@chem.iitb.ac.in
Supporting information for this article is available on the WWW under http://www.eurjic.org or from the author.

in terms of modulating the size and shape of the molecules formed, we have now investigated the reactions of two monoarylphosphate esters, dipp-H_2 and dmpp-H_2 {[(2,6-$Me_2C_6H_3O$)P(O)$(OH)_2$]} with organotin precursors such as Me_2SnCl_2, nBu$_2$SnO, and nBu(O)(OH)·xH$_2$O. The results of this investigation, which describe the synthesis and structural characterization of polymeric as well as cagelike tin phosphates, are reported herein.

Results and Discussion

Synthesis and Characterization of $[Me_2Sn(\mu_3\text{-dipp})]_n$ (1), $[Me_2Sn(\mu\text{-dmpp-H})_2]_n·nH_2O$ (2), and $[Me_2Sn(\mu\text{-dipp-H})_2]_n·nH_2O$ (3)

The reactions of Me_2SnCl_2 with arylphosphates dipp-H_2 and dmpp-H_2 were initially carried out in tetrahydrofuran in the presence of Et_3N as the HCl scavenger under anhydrous conditions at 65 °C. The product obtained by this route in each case was a mixture of compounds, which could not be either separated or completely characterized. Hence, these reactions were carried out at room temperature in ethanol or methanol in the absence of any HCl scavenger. Thus, the reaction between dipp-H_2 and Me_2SnCl_2 in ethanol at 25 °C leads to the formation of $[Me_2Sn(\mu_3\text{-dipp})]_n$ (**1**). On the other hand, the reaction of dmpp-H_2 with Me_2SnCl_2 takes place in methanol to produce $[Me_2Sn(\mu\text{-dmpp-H})_2]_n·nH_2O$ (**2**) (Scheme 1).

It is interesting to note that the equimolar reaction involving dipp-H_2 produces the 1:1 product **1**, while the same reaction under identical conditions involving dmpp-H_2 results in the formation of the 1:2 product **2**. Intrigued by this observation, we investigated the 1:2 reaction between dipp-H_2 and Me_2SnCl_2 in ethanol and found that the reaction proceeds smoothly to yield $[Me_2Sn(\mu\text{-dipp-H})_2]_n·nH_2O$ (**3**). Thus, the stoichiometric control works very well in the case of dipp-H_2 and it is possible to isolate both the 1:1 and 1:2 products (**1** and **3**), while reactions involving dmpp-H_2 do not show any such control and always yield **2** and no $[Me_2Sn(\mu_3\text{-dmpp})]_n$. It appears that because of the smaller aryl substituent on dmpp-H_2, two dmpp-H ligands could be accommodated around tin. On the other hand, due to the larger aryl substituent on dipp-H_2, compound **3** could be obtained only when the reaction was carried out with two equivalents of dipp-H_2, which suggests that steric control plays a significant role in these reactions.

Analytically pure **1** and **2** were directly obtained as single crystals by crystallization of the respective reaction mixtures at room temperature. Compound **3** was obtained as an insoluble powder. The compounds, once formed, were found to be insoluble in all common organic solvents such as hydrocarbons, alcohols, ether, halogenated solvents, and water, probably because of the formation of polymeric structures (vide infra). Hence, the characterization of **1**–**3** could be carried out only in the solid state. The analytical

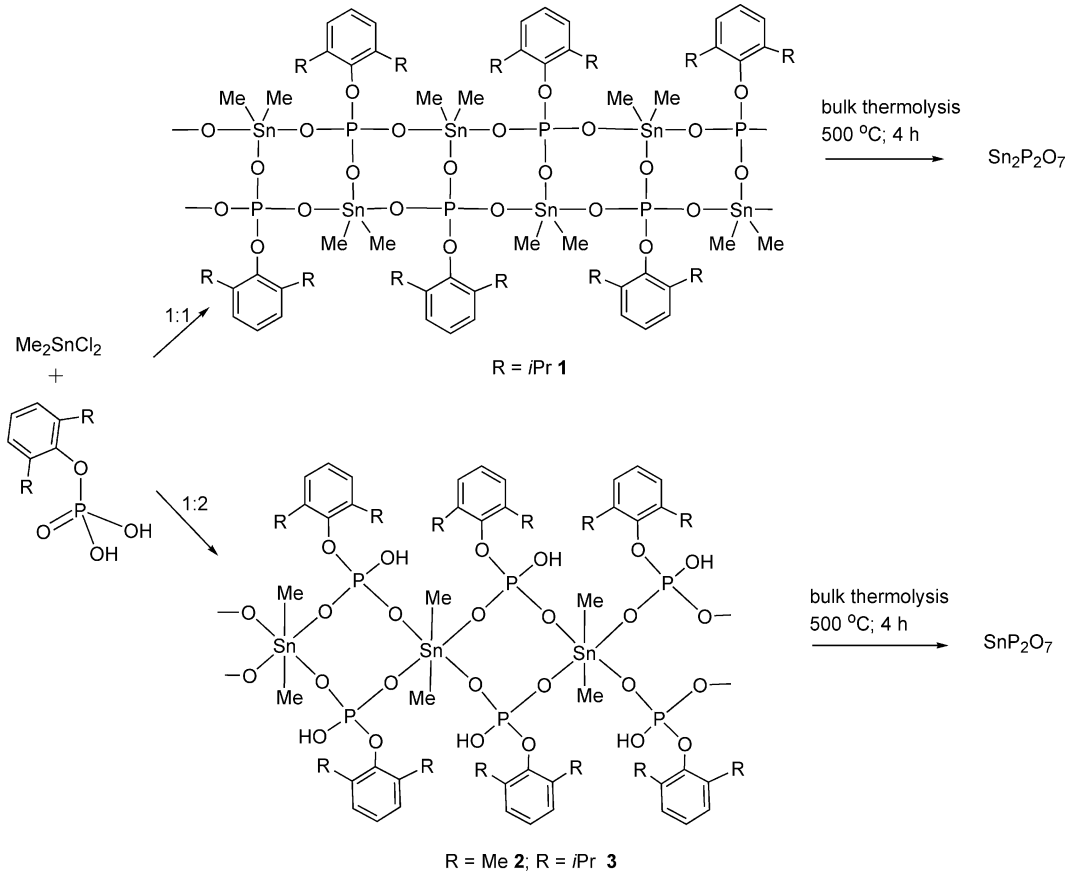

Scheme 1. Synthesis of polymeric organotin phosphates **1**–**3** and their thermolysis.

data obtained for **1** indicates the incorporation of one dipp ligand per tin with a molecular formula of [$Me_2Sn(\mu_3$-dipp)]. The elemental analysis obtained for **2** clearly indicates the presence of two dmpp ligands for each tin with a molecular formula of [$Me_2Sn(\mu_3$-dmpp-H)$_2$]·H_2O. The results from infrared spectroscopy further lend support to this formulation, though a strong broad absorption band at around 2360 cm^{-1} that corresponds to the presence of an unreacted P–OH group in the cases of **2** and **3** is present, while this absorption band is absent in **1**. The IR spectrum of **1** shows broad absorption bands at 1141 and 1031 cm^{-1} that can be assigned to the Sn–O–P symmetric and asymmetric stretching vibrations. The absorption bands occurring at 2967 and 2929 cm^{-1} are due to aliphatic C–H vibrations. Similarly, the IR spectrum of **2** shows absorption bands at 1144 and 1112 cm^{-1} resulting from Sn–O–P symmetric and asymmetric stretching vibrations. The absorption bands at 2956 and 2926 cm^{-1} are due to aliphatic C–H vibrations.

Molecular Structure of [$Me_2Sn(\mu_3$-dipp)]$_n$ (1)

Colorless single crystals of **1** were obtained directly from the reaction mixture after 3 d by slow evaporation of the solvent from the reaction mixture. The compound crystallizes in the monoclinic *I*2/*a* space group. The tin atom in **1** is five-coordinate and is surrounded by two methyl groups and three phosphate oxygen atoms in a trigonal-bipyramidal geometry (Figure 1). The dipp ligand bridges three different tin atoms through its three oxygen atoms in a 3.111 mode (Harris notation).[19] The three phosphate oxygen atoms around the metal ion originate from three different dipp ligands and occupy the two axial and one equatorial positions of the trigonal-bipyramidal polyhedron to form a Sn_2O_3 "T" around the metal. The net result of this coordination mode is the formation of a double-chain polymer made up of fused eight-membered rings (Figure 2). Each of the fused $Sn_2O_4P_2$ rings adopts a sofa conformation, and hence the polymeric double-chain is nonplanar.

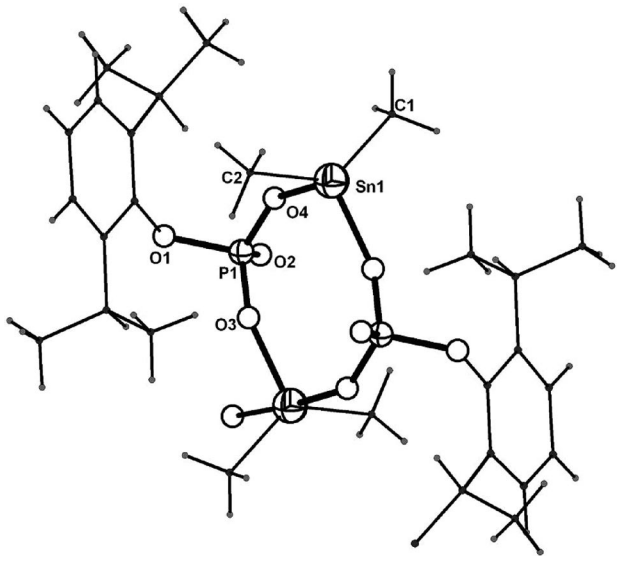

Figure 1. A section of polymeric **1** that illustrates the presence of eight-membered $Sn_2O_4P_2$ rings and the coordination geometry around the tin atom. Selected bond lengths [Å] and angles [°]: Sn1–O2 2.154(6), Sn1–O3 2.022(7), Sn1–O4 2.153(6), P1–O1 1.614(8), P1–O2 1.495(7), P1–O3 1.512(6), P1–O4 1.508(6); O3–Sn1–O4 86.9(2), O3–Sn1–O2 90.0(2), O4–Sn1–O2 176.3(2).

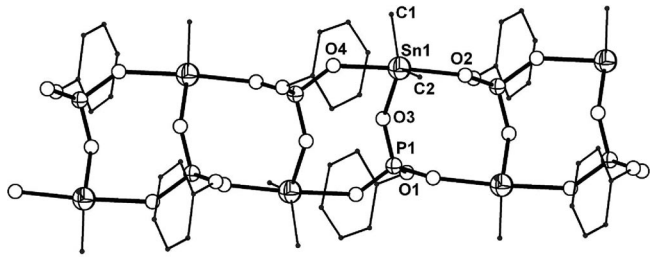

Figure 2. Polymeric structure of **1** in the crystal. The hydrogen atoms and the isopropyl carbon atoms are omitted for clarity.

All the three Sn–O bonds in the molecule are almost of equal length. The P–O(M) bonds [1.495(7)–1.512(6) Å] are shorter than the P–O(C) bond [1.614(8) Å]. The bond angles around the tin atom in **1** do not deviate appreciably from the ideal values expected for a trigonal-bipyramidal geometry. Similarly, the O–P–O angles around the phosphorus atom of the dipp ligand do not vary significantly from the tetrahedral angles.

Molecular Structure of [$Me_2Sn(\mu$-dmpp-H)$_2$]$_n$·nH_2O (2)

Colorless single crystals of **2** were obtained from a methanol/ethanol solution by slow evaporation of the solvent at room temperature. Compound **2** crystallizes in triclinic $P\bar{1}$ space group. The unit cell contains the repeating units of two crystallographically independent tin phosphate polymers. The coordination environment around one of the tin atoms is shown in Figure 3, and the structure of one of the polymeric chains is shown in Figure 4. Every tin atom in the polymeric chain is surrounded by two methyl groups and four oxygen atoms from four different bridging phosphate ligands. In other words, the adjacent dimethyltin units in the chain are linked by the POO^- moiety of two bridging dmpp-H ligands. This results in the formation of $Sn_2O_4P_2$ rings that are connected to each other at the tin centers. The individual eight-membered rings as well as the polymeric chain as a whole are planar, unlike that observed for **1**. The structure of **2** resembles that of the di-*tert*-butyl phosphate copper polymer [Cu(dtbp)$_2$]$_n$, reported by us a few years ago.[20] The major difference between the structure of **2** and [Cu(dtbp)$_2$]$_n$ is the presence of an unionized P–OH group in **2**.

While dipp is tridentate in **1**, the dmpp-H ligand in **2** acts only as a bidentate ligand. Because of this, the P–O(M) bonds [P1–O2 1.483(4), P1–O3 1.502(4), P2–O6 1.521(4), P2–O7 1.507(4) Å] around each phosphorus atom are shorter than the other P–O distances. The P–O(C) bond lengths are the longest [P1–O1 1.589(4), P2–O5 1.584(4) Å], while the P–O(H) distances are of intermediate length [P1–O4 1.559(4), P2–O8 1.562(4) Å]. All the Sn–O distances in the molecule are very similar. While the tin atoms exhibit almost regular octahedral coordination geometries, the

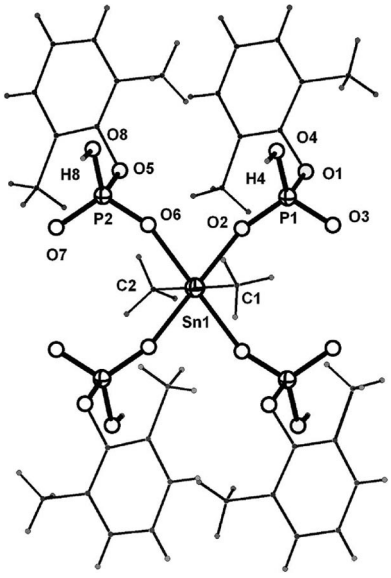

Figure 3. A segment of one of the polymeric chains in **2** that shows the coordination environment around the tin atom. Selected bond lengths [Å] and angles [°]: Sn1–O2 2.215(4), Sn1–O3 2.250(4), Sn1–O6 2.236(4), Sn1–O7 2.197(4), P1–O1 1.589(4), P1–O2 1.483(4), P1–O3 1.502(4), P1–O4 1.559(5), P2–O5 1.584(4), P2–O6 1.521(4), P2–O7 1.507(4), P2–O8 1.562(5); C1–Sn1–O7 88.1(2), C2–Sn1–O7 92.6(2), C1–Sn1–O2 91.7(2), C2–Sn1–O2 87.6(2), C1–Sn1–O6 87.9(2), C2–Sn1–O6 92.1(2), O7–Sn1–O6 94.2(2), O2–Sn1–O6 86.2(2), C1–Sn1–O3 91.7(2), C2–Sn1–O3 88.4(2), O7–Sn1–O3 85.6(2), O2–Sn1–O3 94.0(2), O7–Sn1–O2 179.6(2), O6–Sn1–O3 179.5(2). The repeating unit based on Sn2 has similar bond lengths and angles.

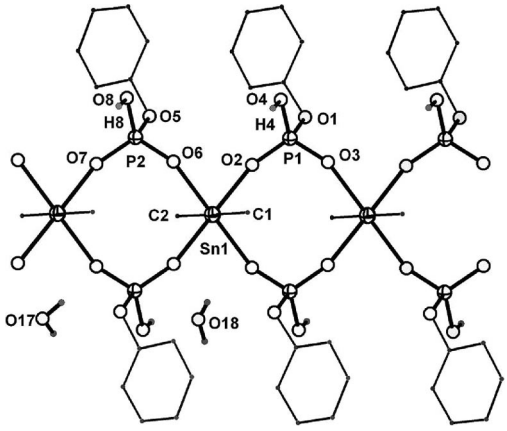

Figure 4. Polymeric chain formation in **2**.

phosphorus centers remain largely tetrahedral. The Sn–O–P angle is quite large (av. Sn–O–P 138.6°).

This unionized P–OH group in **2** acts the source of extensive interchain hydrogen bonding between the polymeric chains, which has been further aided by the presence of lattice water molecules residing between the chains (Figure 5). Although there is no H-bonding between the water molecules, which themselves are arranged in the form of a chain between the two tin phosphate polymeric chains, each water molecule is involved in the formation of four O–H···O hydrogen bonds. In two of these H-bonds, water acts as a donor, while in the other two it acts as the acceptor. Since the H-bonding interactions exist between any two adjacent polymeric chains in the lattice, there is a continuum of H-bonds in the crystal, which explains the complete insolubility of **2** in most solvents.

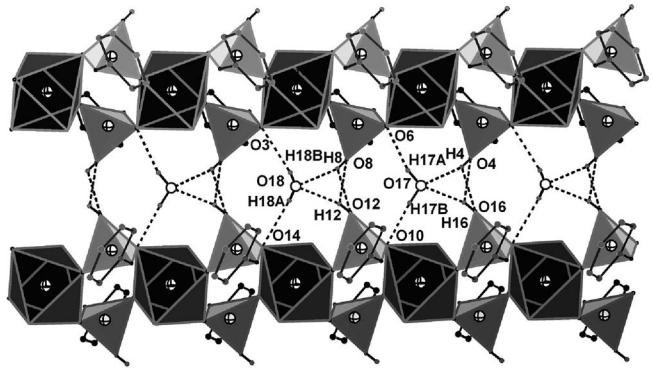

Figure 5. Lattice water aided interchain hydrogen bonding in **2**. The phosphate groups are shown as gray polyhedra, while the tin centers are in the black polyhedra.

Synthesis and Characterization of [nBu$_2$Sn(μ-dipp-H)-(dipp-H)]$_2$ (4)

The reaction between dibutyltin oxide (nBu$_2$SnO) and dipp-H$_2$ in a 1:1 molar ratio takes place in acetone at 25 °C over a period of 2 d and results in the precipitation of a white powder. Crystallization of this white precipitate in toluene at room temperature yields colorless crystals of [nBu$_2$Sn(μ-dipp-H)(dipp-H)]$_2$ (**4**) (Scheme 2). As in the case of the formation of **3** described above, the above reaction does not produce the 1:1 product for any of the stoichiometric conditions employed during the synthesis. Hence, higher yields of **4** were obtained by repeating the reaction in a 1:2 molar ratio of the two reactants.

The composition of **4** could readily be inferred from the analytical data obtained for its single crystals. Unlike compounds **1**–**3**, the *n*-butyl derivative **4** is soluble in most organic solvents and hence could be characterized in solution. The enhanced solubility of **4** could be attributable to the presence of two *n*-butyl groups on each tin atom as well as the formation of a smaller aggregate because of steric reasons (vide infra).

The infrared spectrum of **4** shows a strong and broad absorption band at 2320 cm^{-1} arising from the presence of unreacted P–OH groups on the dipp ligand. The ESI mass spectrum of **4** recorded in a toluene/acetonitrile mixture shows the base peak at m/z = 979.3 that corresponds to the [M – 2dipp]$^+$ fragment. The integrated ^{1}H NMR spectral intensities of the *n*-butyl and the phosphate aryl groups suggest the presence of two dipp-H ligands per tin atom. The resonance appearing at δ = 5.20 ppm is due to the P–OH protons. The ^{31}P NMR spectrum shows two very broad singlets at –7.0 and –12.1 ppm. Because of the very broad nature of the signals, the expected $^{117/119}$Sn satellite peaks could not be observed. Moreover, since the X-ray diffrac-

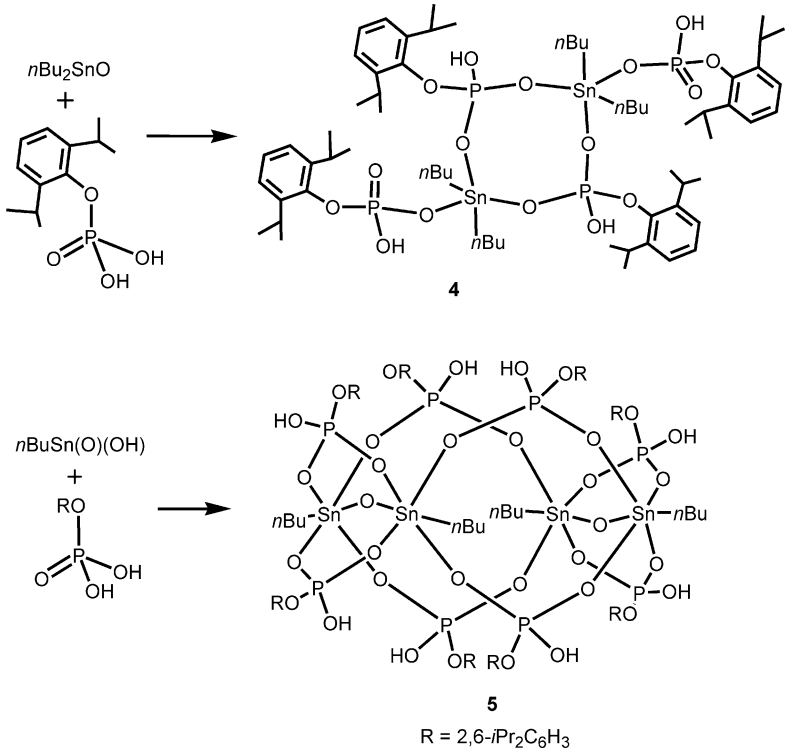

Scheme 2. Synthesis of dimeric and tetrameric organotin phosphates **4** and **5**.

tion studies suggest that the molecule should exhibit a three line spectrum (with a 2:1:1 ratio for dipp-H, dipp-H_2 and dipp ligands, respectively), a variable temperature ^{31}P NMR study was carried out in the temperature range 300–243 K. The spectral pattern, however, remained the same. Thus, the presence of only two ^{31}P NMR signals over the entire temperature range studied suggests that the only two types of dipp-H phosphate ligands exist in the molecule in solution as has been reported for the di-*n*-butyltin methylphosphonate complex by Ribot et al.[15] These observations have further been supported by the presence of a single broad multiplet centered at –258.7 ppm in the ^{119}Sn NMR spectrum of **4**.

Molecular Structure of 4

Compound **4** was crystallized from toluene at room temperature, and colorless single crystals were obtained after 5 d by slow evaporation of the solvent. Compound **4** crystallizes in the triclinic $P\bar{1}$ space group. The asymmetric part of the unit cell has two halves of chemically and crystallographically different tin phosphate molecules (Figure 6). The two molecules of **4** in the unit cell are centrosymmetric dimers based on eight-membered rings containing two five-coordinate tin atoms and two phosphate ligands that bridge the tin atoms. The tin atoms in both the molecules exhibit a trigonal-bipyramidal environment. Apart from the two butyl groups and the two bridging phosphate ligands, each tin is surrounded by an additional terminal phosphate ligand.

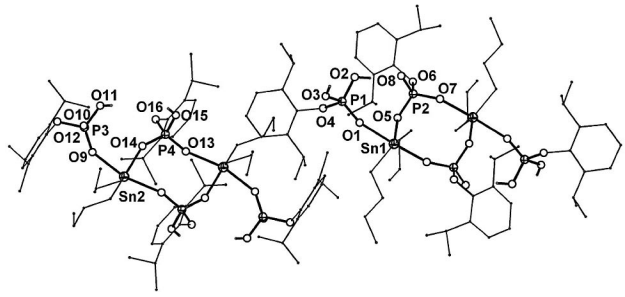

Figure 6. Molecular structure of [nBu$_2$Sn(dipp-H)(μ-dipp-H)]$_2$ (**4**). Selected bond lengths [Å] and angles [°]: Sn1–O5 2.027(2), Sn1–O7 2.156(2), Sn1–O1 2.259(2), Sn2–O14 2.036(2), Sn2–O9 2.148(2), Sn2–O13 2.178(2), P1–O1 1.483(2), P1–O2 1.532(3), P1–O3 1.538(3), P1–O4 1.571(2), P2–O7 1.498(2), P2–O6 1.516(2), P2–O5 1.539(2), P2–O8 1.587(3), P3–O10 1.497(3), P3–O9 1.499(2), P3–O11 1.553(3), P3–O12 1.583(2), P4–O13 1.494(2), P4–O14 1.500(3), P4–O15 1.536(3), P4–O16 1.588(3), O2–H2 0.84(6), O3–H3 0.75(4), O7–P2(#1) 1.498(2), O8–C21 1.422(4), O11–H11 0.71(4), O14–P4(#2) 1.500(3), O15–H15 0.63(3); O5–Sn1–O7 88.55(9), O5–Sn1–O1 86.65(9), O7–Sn1–O1 175.09(9), O14–Sn2–O9 82.84(9), O14–Sn2–O13 82.45(9), O9–Sn2–O13 164.98(9), O1–P1–O2 113.8(2), O1–P1–O3 114.1(2), O2–P1–O3 108.2(2), O1–P1–O4 109.3(1), O2–P1–O4 106.3(2), O3–P1–O4 104.5(1), O7(#1)–P2–O6 113.3(1), O7(#1)–P2–O5 112.2(1), O6–P2–O5 109.9(1), O7(#1)–P2–O8 105.8(1), O6–P2–O8 109.9(1), O5–P2–O8 105.4(1), O10–P3–O9 115.0(2), O10–P3–O11 111.1(2), O9–P3–O11 111.5(2), O10–P3–O12 107.4(1), O9–P3–O12 108.0(1), O11–P3–O12 103.0(2), O13–P4–O14(#2) 117.7(1), O13–P4–O15 109.9(2), O14(#2)–P4–O15 109.9(2), O13–P4–O16 108.3(1), O14(#2)–P4–O16 104.3(1), O15–P4–O16 107.0(2), P1–O1–Sn1 149.9(2), P2–O5–Sn1 125.0(1), P2(#1)–O7–Sn1 143.0(2), P3–O9–Sn2 138.3(2), P4–O13–Sn2 155.4(2), P4(#2)–O14–Sn2 149.8 (2).

The two independent molecules of **4** in the unit cell, however, differ from each other in terms of the number of undissociated protons on the phosphate ligands. For example, the bridging phosphate ligands in molecule A (Sn1) have lost both the acidic protons (dipp), while the terminal phosphate ligand is completely undissociated (dipp-H_2). On the other hand, in molecule B (Sn2), the bridging as well as the terminal phosphate ligands are monodissociated (dipp-H).[21] This can be readily seen from the differences in the P2–O6 [1.516(2) Å] and P4–O16 distances [1.588(3) Å]. Thus, the composition of **4** in the crystal can best be described as [{nBu$_2$Sn(μ-dipp)(dipp-H_2)}$_2${nBu$_2$Sn(μ-dipp-H)(dipp-H)}$_2$], although in solution there are no totally undissociated or doubly dissociated phosphate ligands, as evidenced by variable-temperature ^{31}P NMR spectroscopy. A closer look at the {nBu$_2$Sn(μ-dipp)(dipp-H_2)}$_2$ part of **4** reveals that one of the P–OH groups [O2] of the terminal ligand is pointed towards the phosphoryl group of the bridging ligand [O6], which facilitates the formation of a strong P–O–H···O=P intramolecular hydrogen bond. This proton, sandwiched between the P–O groups, prefers the terminal oxygen atom in the solid state, while it stays on the bridging phosphate oxygen atom in solution, thus producing only one set of ^{31}P NMR signals.

Apart from the above-mentioned O2–H···O6 intramolecular hydrogen bond between the terminal and bridging phosphate ligands in molecule A [Sn1], there are additional intermolecular O–H···O hydrogen bonds that results in the formation of the H-bonded polymeric chain, as shown in Figure 7 (bottom). In molecule B, there are no intramolecular hydrogen bonds, but intermolecular hydrogen bonds are exclusively formed, as shown in Figure 7 (top), to produce a ladder-type structure. This structure contains a covalent eight-membered ring, a hydrogen-bonded eight-membered ring, and a hydrogen-bonded six-membered ring as the repeating unit.

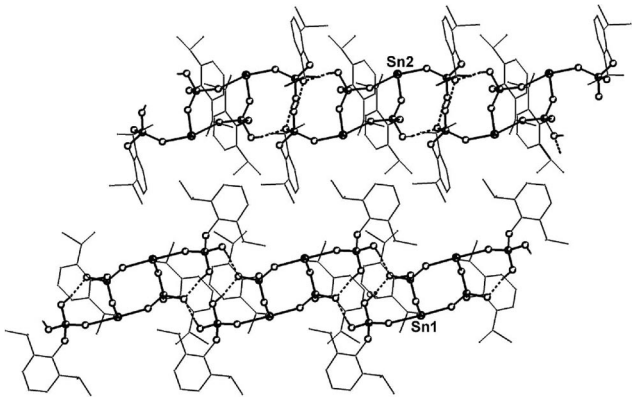

Figure 7. Hydrogen-bonding polymeric chains of [{nBu$_2$Sn(μ-dipp)(dipp-H_2)}$_2${nBu$_2$Sn(μ-dipp-H)(dipp-H)}$_2$] (**4**). The H-bonding pattern observed for the bottom (Sn1) and top chains (Sn2) are different. (Phenyl hydrogen atoms, and *n*-butyl and isopropyl hydrogen atoms are removed for clarity).

Synthesis and Characterization of [(nBuSn)$_4$(O)$_2$(dipp-H)$_8$] (5)

The reaction of *n*-butylstannoic acid with dipp-H_2 was carried out by using a procedure that is very similar to the synthesis of **4**. The reaction of 2 equiv:dipp-H_2 with *n*-butylstannoic acid in acetone at room temperature over a few days produces [(nBuSn)$_4$(O)$_2$(dipp-H)$_8$] (**5**). Like **4**, compound **5** is also soluble in common organic solvents. The elemental analysis of **5** indicates the presence of two dipp ligands per [nBuSn] unit (Scheme 2).

The IR spectrum of **5** shows absorption bands at 1176 and 1150 cm^{-1} corresponding to presence of Sn–O–P symmetric and asymmetric stretching frequencies. The broad absorption peak observed at 2329 cm^{-1} is due to the presence of unionized P–OH groups on the phosphate ligands. The absorption bands at 2964 and 2931 cm^{-1} are due to aliphatic C–H vibrations. In the ESI mass spectrum of compound **5**, the peak observed at m/z = 2431.5 corresponds to the loss of one dipp ligand, one *n*-butyl group, and two –OH ligands from the molecular ion. Further loss of the additional dipp ligand produces a peak at m/z = 2192.2. The base peak at m/z = 1551.2 is for the [M – 4dipp – 3nBu – 2OH]$^+$ fragment.

In the ^{1}H NMR spectrum, compound **5** shows a triplet at around 7.23–7.30 ppm and a doublet at around 7.15–7.20 ppm for the aryl protons. The broad peak centred at δ = 4.75 ppm corresponds to the resonance of the P–OH protons. As expected, methine protons show a multiplet in the region 3.30–3.60 ppm, while the methyl of the isopropyl groups presents a doublet in the region 1.33–1.41 ppm. Multiplets are observed in the appropriate region for the methyl and methylene protons of the *n*-butyl groups with expected intensities. In the ^{31}P NMR spectrum, there are two singlet resonances at –10.56 and –19.26 ppm with the $^{117/119}$Sn satellites ($^2J_{SnP}$ = 283.2 and 226.2 Hz, respectively). The spectral pattern and the chemical shift values are similar to those reported for [(nBuSn)$_4$(O)$_2$(tbp-H)$_8$][11] or [(PhCH$_2$Sn)$_4$(O)$_2$(tbp-H)$_8$][14] (tbp-H_2 = *tert*-butylphosphonic acid), which suggests that **5** will also have a similar molecular structure. Thus, the observed ^{31}P NMR spectral pattern of **5** is consistent with the molecular formula [(nBuSn)$_4$(O)$_2$(dipp-H)$_8$]$_n$, in which four dipp-H ligands are in one environment, while the remaining four dipp-H ligands are in a different environment, at least in solution. The ^{13}C NMR spectrum further confirms this solution structure for **5** with the presence of only thirteen signals in the expected regions. The ^{119}Sn NMR spectrum of **5** shows a single multiplet centered at –641.5 ppm, which arises from the four chemically equivalent tin atoms in the molecule that are coupled to two different types of phosphorus centers.

Molecular Structure of 5

Compound **5** was crystallized from CH_2Cl_2/toluene at 5 °C. The colorless single crystals obtained after 5 d were found to crystallize in the monoclinic *C*2/*c* space group. The molecule is centrosymmetric and contains four tin atoms and eight phosphate molecules. The core structure of **5** es-

sentially resembles the *tert*-butylphosphonate tin clusters $[(n\text{BuSn})_4(O)_2(\text{tbp-H})_8]$[11] or $[(PhCH_2Sn)_4(O)_2(\text{tbp-H})_8]$[14] (Figure 8). However, the overall solid-state structure of **5** is clearly different from its solution structure or from the solid-state structures reported for $[(n\text{BuSn})_4(O)_2(\text{tbp-H})_8]$[11] or $[(PhCH_2Sn)_4(O)_2(\text{tbp-H})_8]$.[14] While the phosphonate clusters are built around two RSn–O–SnR units that are held together by eight tbp-H phosphonate ligands,[11,14] this unit in **5** is a RSn–OH–SnR group. Because of the presence of an OH^- group instead of an O^{2-} anion, two out of the total eight phosphate ligands are doubly ionized. Thus, the cluster **5** contains two dipp and six dipp-H ligands. The P1 and P4 (or P1′ and P4′) phosphate groups hold the tin atoms within the Sn–OH–Sn units together, while the two dipp ligands (P2 and P2′) and two dipp-H ligands (P3 and P3′) bridge the two Sn–OH–Sn units across to eventually result in a cubane-like structure.

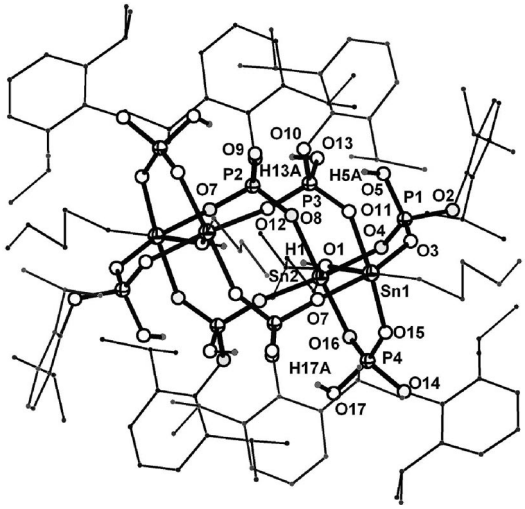

Figure 8. Molecular structure of **5**. Selected bond lengths [Å] and angles [°]: Sn1–O3 2.070(2), Sn1–O7 2.082(2), Sn1–O15 2.097(2), Sn1–O11 2.107(2), Sn1–O1 2.109(2), Sn2–O16 2.086(2), Sn2–O4 2.090(2), Sn2–O8 2.092(2), Sn2–O1 2.103(2), Sn2–O12 2.118(2), P1–O3 1.501(2), P1–O4 1.509(2), P1–O5 1.543(2), P1–O2 1.566(2), P2–O8 1.505(2), P2–O7 1.511(2), P2–O9 1.527(2), P2–O6 1.580(2), P3–O12 1.499(2), P3–O11 1.511(2), P3–O13 1.540(2), P3–O10 1.582(2), P4–O15 1.501(2), P4–O16 1.502(2), P4–O17 1.535(3), P4–O14 1.570(2); O3–Sn1–O7 164.77(8), O3–Sn1–O15 89.75(9), O7–Sn1–O15 92.94(9), O3–Sn1–O11 87.10(9), O7–Sn1–O11 87.55(8), O15–Sn1–O11 169.46(8), O3–Sn1–O1 81.83(9), O7–Sn1–O1 83.54(9), O15–Sn1–O1 84.19(8), O11–Sn1–O1 85.40(8), O16–Sn2–O4 90.20(9), O16–Sn2–O8 168.53(9), O4–Sn2–O8 88.70(9), O16–Sn2–O1 85.16(9), O4–Sn2–O1 83.53(9), O8–Sn2–O1 83.37(8), O16–Sn2–O12 90.81(9), O4–Sn2–O12 161.36(8), O8–Sn2–O12 86.63(8), O1–Sn2–O12 78.00(9).

Apart from the fact that there are no hydrogen atoms found near O9, the P2–O9 distance is also considerably shorter [1.527(2) Å] than the P1–O5, P3–O13, and P4–O17 distances [1.543(2), 1.540(3), 1.535(3) Å, respectively]. Further, the hydrogen atom on O1 can easily be located on the difference Fourier map, and its inclusion in the refinement results in an excellent convergence for the positional and thermal parameters. Hence, it can be concluded that **5**, in the solid state, has the structure $[n\text{Bu}_4\text{Sn}_4(\mu\text{-OH})_2(\mu\text{-dipp-H})_6(\mu\text{-dipp})_2]$, while in solution it retains the structure $[n\text{Bu}_4\text{Sn}_4(\mu\text{-O})_2(\mu\text{-dipp-H})_8]$.[22]

Since the X-ray diffraction studies suggest the presence of two totally dissociated dipp ligands, the ^{31}P NMR spectrum of **5** was one again investigated in the temperature range 300–243 K in order to see whether the solid-state structure is also frozen in solution at lower temperature. The results of this investigation, however, clearly show no spectral change in the entire temperature range. It appears that the transformation of one form to the other seems to be a facile process when compound **5** is dissolved in $CDCl_3$, which is aided by the presence of extensive intramolecular hydrogen bonding between the P–OH groups and other potential hydrogen-bond donors and acceptors within the molecule (Figure 9).

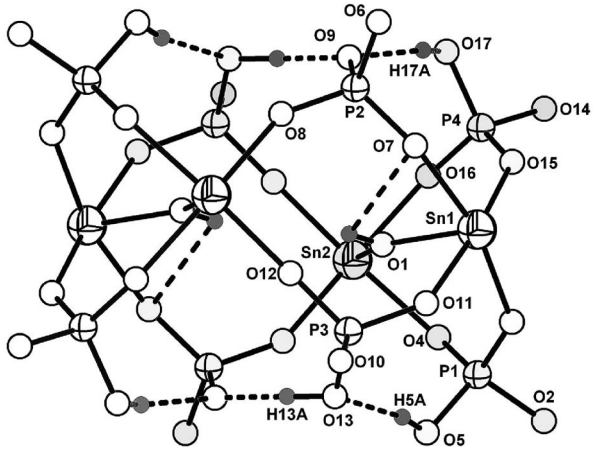

Figure 9. Core structure of **5** that shows six phosphate monoanions and two phosphate dianions. The hydrogen bonds formed by the undissociated hydrogen atoms are shown as broken lines.

Thermal Studies

The thermal analysis (TGA) of **1** showed that the sample is stable on heating up to 350 °C. Subsequent heating in the region 350–500 °C leads to a major weight loss (59%), which corresponds to the loss of both methyl and 2,6-diisopropylphenyl groups. The residue left at this point roughly corresponds to the formation of $Sn_2P_2O_7$ (≈ 35%). In order to confirm the formation of $Sn_2P_2O_7$, a bulk themolysis of **1** at 500 °C was carried out for 4 h. The final residue obtained was examined by PXRD and was indeed found to be $Sn_2P_2O_7$.[23]

In the case of **2**, the TGA studies showed that the loss of organic moiety takes place very slowly in the temperature range 300–500 °C, probably because of the presence of two phosphate ligands per metal atom. The weight of the residue left after condensation of all free –OH groups corresponds to the formation of SnP_2O_7 in this case. Compound **3** undergoes two weight losses; the initial loss at around 100 °C corresponds to the removal of the lattice water molecule. Subsequently, between 200 and 400 °C, the organic substituents are lost, and the final decomposition product

that remains just above 500 °C is formulated as SnP_2O_7. An independent thermolysis of the bulk samples of **2** and **3** at 500 °C for 4 h followed by PXRD examination revealed that the final decomposition product indeed is SnP_2O_7.[24]

The final decomposition products obtained at ca. 500 °C for the above thermolysis studies were found to be phase pure. However, if the decomposition was continued beyond 800 °C, P_2O_5 is lost, which leads to the formation of tin oxide(s), as was observed for several metal phosphates prepared by us using molecular precursor routes.[25] The formation of $Sn_2P_2O_7$ in the case of **1** and SnP_2O_7 in the case of **2** clearly demonstrate the importance of designing suitable precursors with an appropriate metal/phosphate ligand ratio in order to obtain phase-pure ceramic phosphates. In the thermolysis of both **4** and **5**, which also contain a Sn/P ratio of 1:2, **4** and **5** neatly decompose to yield SnP_2O_7 as in the case of **2** and **3**.

Conclusions

We have shown that a variety of oligomeric and polymeric structures of tin phosphates can be synthesized by a proper choice of organotin precursor and organophosphate ester as the reactant. When the organic substituent on the tin atom is a methyl group, invariably a polymeric material (compounds **1**–**3**) is obtained as the product. The nature of polymer formed seems to further depend on the organic substituent on the phosphate oxygen atom. While the 2,6-diisoprpyl group on the phosphorus atom prefers the formation of a 1:1 polymer **1** with a ladder structure, the presence of the smaller 2,6-dimethylphenyl substituent invariably results in the formation of a 1:2 polymer **2**. The change in the organic substituent on the tin atom to the (bulkier) *n*-butyl group completely impedes polymer formation, and in this case only a dimeric phosphate that contains both bridging and terminal phosphate ligands (compound **4**) can be obtained. Decreasing the organic content on tin, by choosing *n*BuSn(O)(OH) as the precursor, leads to the isolation of a 3D cage structure **5** and not to a ring or polymeric structure. In the cases in which it is possible to obtain soluble compounds, it has been shown that the solution structures differ somewhat from the solid-state structures. These changes often involve the movement of acidic protons within the molecule, often aided by strong intramolecular hydrogen bonds. This clearly suggests that it would be possible to obtain more structural types of tin phosphates by a careful variation of the starting materials. Finally, the different tin/phosphorus ratios found in the compounds reported herein prompted the investigation of their utilization as precursors for tin phosphate ceramic materials. Because of the 1:1 ratio of Sn/P in **1**, the thermolysis leads to the isolation of $Sn_2P_2O_7$, while the thermolysis of compounds **2**–**5** proceeds to form SnP_2O_7.

Experimental Section

General: All reactions were carried out in the presence of air in a beaker; however, precautions were taken to avoid contact of all tin compounds. Commercially available starting materials such as dimethyltin dichloride (Aldrich), diphenyltin dichloride (Aldrich), *n*-butylstannoic acid(Aldrich), di-*n*-butyltin oxide (Aldrich) were used as received. The ^1H (Me_4Si internal standard), ^{31}P (85% H_3PO_4 external standard), and ^{119}Sn (Ph_4Sn external standard) NMR spectra were recorded on a Varian VXR 400S spectrometer. Infrared spectra were obtained from a Nicolet Impact-400 FT-IR spectrometer. Microanalyses were performed on a Thermo Finnigan (FLASH EA 1112) or a Carlo Eraba 1106 microanalyzer. Thermogravimetric analysis was carried out at IIT, Bombay, on a Perkin–Elmer thermal analysis system, under a stream of nitrogen gas. Powder X-ray diffraction data were obtained with a Philips X′Pert Pro X-ray diffraction system by using monochromated Cu-$K_{\alpha1}$ radiation (λ = 1.5406 Å).

Synthesis of 1: A solution of dipp-H_2 (258 mg, 1 mmol) in ethanol (25 mL) was added to a solution of Me_2SnCl_2 (220 mg, 1 mmol) in ethanol (25 mL). The reaction mixture was stirred for 6 h. The solution was filtered and left to crystallize at room temperature. Colorless crystals of **1** were formed from this solution after 3 d. Yield: 366 mg (90% based on Me_2SnCl_2). M.p.: >250 °C. $C_{14}H_{23}O_4PSn$ (M_r = 404.98): calcd. C 41.52, H 5.72; found C 41.69, H 5.22. IR (KBr): $\tilde{\nu}$ = 3431 (br.), 3057 (w), 3021 (w), 2967 (m), 2929 (m), 2868 (w), 1639 (w), 1466 (w), 1445 (vs), 1405 (w), 1361 (w), 1254 (w), 1200 (w), 1192 (w), 1144 (w), 1088 (w), 1046 (w), 1031 (w), 926 (s), 881 (w), 796 (w), 772 (w), 750 (w), 666 (s), 601 (w), 581 (w), 539 (w) cm^{-1}. TGA: temperature range (weight loss): 350–450 °C (59%).

Synthesis of 2: A solution of dmpp-H_2 (202 mg, 1 mmol) in methanol (25 mL) was added to a solution of Me_2SnCl_2 (220 mg, 1 mmol) in methanol (25 mL). The reaction mixture was stirred for 6 h. The solution was filtered; ethanol (10 mL) was added, and the solution was left to crystallize at room temperature. Colorless crystals of **2** were formed from this solution after 5 d. Yield: 265 mg (47% based on Me_2SnCl_2). M.p.: >250 °C. $C_{18}H_{28}O_9P_2Sn$ (M_r = 569.04): calcd. C 37.99, H 4.96; found C 37.84, H 4.72. IR (KBr): $\tilde{\nu}$ = 3432 (br.), 3021 (w), 2956 (w), 2926 (m), 2846 (w), 1621 (br.), 1476 (s), 1269 (w), 1204 (w), 1179 (w), 1144 (vs), 1112 (vs), 1011 (vs), 942 (w), 917 (s), 781 (vs), 738 (w), 660 (w), 620 (w), 586 (w), 525 (w) cm^{-1}. TGA: temperature range (weight loss): 155–252 (1%), 252–411 (34%), 411–604 °C (12%).

Synthesis of 3: A solution of dipp-H_2 (516 mg, 2 mmol) in ethanol (25 mL) was added to a solution of Me_2SnCl_2 (220 mg, 1 mmol) in ethanol (25 mL). The reaction mixture was stirred for 6 h. The solution was filtered and left to crystallize at room temperature. A colorless amorphous solid precipitated from this solution after 3 d. Yield: 238 mg (35% based on Me_2SnCl_2). M.p.: >250 °C. $C_{26}H_{44}P_2O_8Sn$ (M_r = 681.29): C 45.84, H 6.51; found C 46.39, H 6.18. IR (KBr): $\tilde{\nu}$ = 3618 (w), 3430 (br.), 3060 (w), 2967 (s), 2934 (w), 2873 (w), 2300 (br.), 1934 (w), 1617 (br.), 1462 (w), 1437 (m), 1386 (w), 1365 (w), 1335 (w), 1298 (w), 1256 (w), 1209 (w) 1173(s), 1096 (w), 1073 (m), 1049 (s), 995 (vs), 968 (s), 930 (w), 916 (w), 798 (w), 775 (w), 751 (w), 658 (w), 599 (w), 522 (m), 539 (w) cm^{-1}. TGA: temperature range (weight loss): 70–120 (3%), 120–500 °C (62%).

Synthesis of 4: A solution of dipp-H_2 (516 mg, 2 mmol) in acetone (25 mL) was added to a solution of nBu_2SnO (249 mg, 1 mmol) in acetone (25 mL). The reaction mixture was stirred for 2 h. The solution was filtered. The precipitate obtained from the filtrate after 2 d was dissolved in toluene, and the solution was left to crystallize at room temperature. Colorless crystals of **4** were formed from this solution after 5 d. Yield: 318 mg (43% based on nBu_2SnO). M.p.: 193–195 °C. $C_{64}H_{108}O_{16}P_4Sn_2$ (M_r = 1496.46):

Table 1. Crystal data for **1**, **2**, **4**, and **5**.

	1	**2**	**4**	**5**
Formula	$C_{14}H_{23}O_4PSn$	$C_{18}H_{28}O_9P_2Sn$	$C_{64}H_{108}O_{16}P_4Sn_2$	$C_{112}H_{180}O_{34}P_8Sn_4$
F_w	404.98	569.04	1494.76	2793.08
T [K]	150(2)	150(2)	150(2)	150(2)
Wavelength [Å]	0.71073	0.71073	0.71073	0.71073
Crystal system	monoclinic	triclinic	triclinic	monoclinic
Space group	$I2/a$	$P\bar{1}$	$P\bar{1}$	$C2/c$
a [Å]	11.2029(10)	10.026(2)	10.4259(2)	28.6248(5)
b [Å]	25.342(2)	15.4266(17)	14.5000(4)	21.9667(4)
c [Å]	13.1541(12)	16.1250(18)	24.5511(6)	21.2309(3)
α [°]	90	66.927(2)	94.583(2)	90
β [°]	110.209(9)	89.987(6)	91.475(2)	95.142(1)
γ [°]	90	80.720(5)	97.696(2)	90
V [Å^3]	3504.6(5)	2259.1(6)	3663.84(15)	13296.1(4)
Z	8	4	2	4
$D_{calcd.}$ [Mg m^{-3}]	1.535	1.673	1.355	1.395
Abs. coeff. [mm^{-1}]	1.558	1.319	0.829	0.909
$F(000)$	1632	1152	1560	5776
Crystal size [mm]	0.40 × 0.25 × 0.15	0.33 × 0.26 × 0.21	0.33 × 0.26 × 0.21	0.34 × 0.31 × 0.28
θ range [°]	3.09–25.00	3.12–25.00	2.97–25.00	2.95–25.00
Data (R_{int})	3085 (0.1625)	7896 (0.0216)	12763 (0.0405)	11676 (0.0367)
Completeness to 2θ [%]	99.6	99.0	98.8	99.7
Restraints/parameters	0/187	0/565	0/791	42/775
GoF on F^2	0.966	0.915	1.049	1.109
R_1 [$I > 2\sigma(I)$]	0.0679	0.0209	0.0363	0.0323
wR_2 [$I > 2\sigma(I)$]	0.1141	0.0543	0.0736	0.0620
$R1$ (all data)	0.1555	0.0704	0.0629	0.0481

calcd. C 51.42, H 7.28; found C 50.95, H 7.76. IR (KBr): $\tilde{\nu}$ = 3417 (br.), 3065 (w), 2965 (vs), 2923 (m), 2870 (m), 2320 (br.), 1931 (br.), 1860 (w), 1639 (br.), 1464 (s), 1440 (m), 1383 (w), 1362 (w), 1335 (m), 1257 (s), 1176 (s), 1135 (s), 1111 (w), 1046 (w), 992 (s), 965 (m), 882 (w), 798 (w), 772 (s), 750 (m), 716 (w), 664 (w), 622 (w), 595 (w), 541 (w), 526 (w), 508 (w) cm^{-1}. ^{1}H NMR (C_6D_6, 400 MHz): δ = 0.8–1.0 (s, 3 H, *n*Bu-CH$_3$), 1.12–1.50 (d, $^3J_{HH}$ = 6.0 Hz, 3 H, *i*Pr-CH$_3$), 1.2–1.5 (m, 2 H, *n*Bu-C*H*$_2$), 3.35–3.50 (m, 2 H, *i*Pr-C*H*), 5.20–5.30 (s, 1 H, P-OH), 7.0–7.1 (s, 3 H, Ar-H) ppm. ^{31}P NMR (C_6D_6, 162 MHz): δ = –7.0, –12.1 ppm. ^{119}Sn NMR (C_6D_6): δ = –285.7 ppm. Mass spectrum (ESI = 70 eV): *m*/*z* = 979 [M – 2dipp]$^+$, 749.3 [M – 2dipp – SnBu$_2$]$^+$ and 491.1 [M – 3dipp – SnBu$_2$]$^+$. TGA: temperature range (weight loss): 172–252 (18%), 252–415 °C (46%).

Synthesis of 5: A solution of dipp-H$_2$ (516 mg, 2 mmol) in acetone (25 mL) was added to a solution of *n*BuSn(O)(OH)·*x*H$_2$O (204 mg, ≈1 mmol) in acetone (25 mL). The reaction mixture was stirred for 2 h, filtered, and the clear solution was left standing on the benchtop. The precipitate formed from this solution after 2 d was dissolved in CH$_2$Cl$_2$/toluene, and the solution was left to crystallize at room temperature. Colorless crystals of **5** were obtained after 5 d. Yield: 117 mg (33% based on dipp-H$_2$). M.p.: 211–213 °C. $C_{112}H_{180}O_{34}P_8Sn_4$ (M_r = 2793.08): calcd. C 48.16, H 6.50; found: C 48.66, H 7.31. IR (KBr): $\tilde{\nu}$ = 3538 (br.), 3423 (br.), 32089 (br.), 3060 (w), 3027 (w), 2964 (vs), 2931 (s), 2871 (s), 2329 (br.), 1928 (w), 1860 (w), 1650 (br.), 1465 (w), 1439 (s), 1383 (w), 1362 (w), 1335 (m), 1257 (m), 1176 (s), 1150 (s), 1123 (w), 1108 (w), 1092 (w), 1048 (w), 1012 (w), 986 (s), 936 (w), 882 (w), 872 (w), 795 (w), 769 (w), 750 (w), 685 (w), 659 (w), 625 (w), 595 (w), 548 (w), 529 (w), 510 (w), 458 (w) cm^{-1}. ^{1}H NMR (CDCl$_3$, 400 MHz): δ = 0.70–0.80 (t, $^3J_{HH}$ = 6.4 Hz, 3 H, *n*Bu-CH$_3$), 1.01–1.11 (m, 2 H, *n*Bu-CH$_2$), 1.11–1.19 (m, 2 H, *n*Bu-CH$_2$), 1.33–1.41 (d, $^3J_{HH}$ = 3.2 Hz, 3 H, *i*Pr-CH$_3$), 1.80–1.87 (m, 2 H, *n*Bu-CH$_2$), 3.30–3.60 (m, 2 H, *i*Pr-CH), 4.75–4.85 (t, $^2J_{PH}$ = 6.3 Hz, 1 H, P-OH), 7.15–7.20 (d, $^3J_{HH}$ = 5.6 Hz, 2 H, Ar-H), 7.23–7.30 (t, $^3J_{HH}$ = 5.6 Hz, 1 H, Ar-H) ppm. ^{13}C NMR (CDCl$_3$, 101 MHz): δ = 146.9 (s, C, Ar-C1), 140.8 (s, C, Ar-C2), 123.9 (s, C, Ar-C3), 140.5 (s, C, Ar-C4), 146.5 (s, C, Ar-C5), 125.5 (s, C, Ar-C6), 26.2 (s, C, *i*Pr-CA), 26.9 (s, C, *i*Pr-CB), 26.3 (s, C, *i*Pr-CC), 28.1 (s, C, *n*Bu-C$_a$), 23.5 (s, C, *n*Bu-C$_b$), 23.3 (s, C, *n*Bu-C$_c$), 13.7 (s, C, *n*Bu-C$_d$) ppm. ^{31}P NMR (CDCl$_3$, 162 MHz): δ = –10.6 ($^2J_{SnP}$ = 283.2 Hz), –19.3 ($^2J_{SnP}$ = 226.2 Hz) ppm. ^{119}Sn NMR (CDCl$_3$): δ = –641.5 ppm. Mass spectrum (ESI = 70 eV): *m*/*z* = 2431.5 [M – dipp – Bu – 2OH]$^+$, 2192.2 [M – 2dipp – Bu – 2OH]$^+$ and 1551.2 [M – 4dipp – 3Bu – 2OH]$^+$. TGA: temperature range (weight loss):78–146 (3%), 146–265 (20%), 265–505 °C (40%).

Single-Crystal X-ray Studies: Intensity data for all four samples were collected on a Oxford XCalibur CCD diffractometer. All calculations were carried out with the programs in the WinGX module.[26] The structure solution was achieved by direct methods in most cases using SIR-92 as implemented in WinGX.[27] The final refinement of the structure was carried out by using full least-squares methods on F^2 with SHELXL-97.[28] Selected crystal data are given Table 1. CCDC-666770, -666771, -666772 and -666773 contain the supplementary crystallographic data for this paper. These data can be obtained free of charge from The Cambridge Crystallographic Data Centre via www.ccdc.cam.ac.uk/data_request/cif.

Supporting Information (see footnote on the first page of this article): Characterization data for compounds **1**–**5** is presented.

Acknowledgments

This work was supported by DST, New Delhi, in the form of a Swarnajayanti Fellowship. S. S. thanks the CSIR, New Delhi for a research fellowship. We thank the Single Crystal X-ray Diffraction National Facility at IIT-Bombay for the intensity data.

[1] For example, see: a) , R. Murugavel, A. Voigt, M. G. Walawalkar, H. W. Roesky, *Chem. Rev.* **1996**, *96*, 2205; b) R. Murugavel, V. Chandrasekhar, H. W. Roesky, *Acc. Chem. Res.* **1996**, *29*, 183; c) M. G. Walawalkar, H. W. Roesky, R. Murugavel, *Acc. Chem. Res.* **1999**, *32*, 117.

[2] R. Murugavel, M. G. Walawalkar, M. Dan, H. W. Roesky, C. N. R. Rao, *Acc. Chem. Res.* **2004**, *37*, 763.

[3] R. Murugavel, S. Kuppuswamy, R. Boomishankar, A. Steiner, *Angew. Chem. Int. Ed.* **2006**, *45*, 5536.

[4] R. Murugavel, S. Kuppuswamy, *Angew. Chem. Int. Ed.* **2006**, *45*, 7022.

[5] R. Murugavel, S. Shanmugan, *Chem. Commun.* **2007**, 1257.

[6] R. R. Holmes, *Acc. Chem. Res.* **1989**, *22*, 190.

[7] a) V. Chandrasekhar, K. Gopal, P. Thilagar, *Acc. Chem. Res.* **2007**, *40*, 420; b) V. Chandrasekhar, S. Nagendran, V. Baskar, *Coord. Chem. Rev.* **2002**, *235*, 1.

[8] Reviews: a) E. R. T. Tiekink, *Appl. Organomet. Chem.* **1991**, *5*, 1; b) E. R. T. Tiekink, *Trends Organomet. Chem.* **1994**, *1*, 71.

[9] G. Prabusankar, R. Murugavel, *Organometallics* **2004**, *23*, 5644.

[10] a) Y. Yamamoto, N. Asao, *Chem. Rev.* **1993**, *93*, 2207; b) J. Beckmann, D. Dakternieks, A. Duthie, F. S. Kuan, K. Jurkschat, M. Schuermann, E. R. T. Tiekink, *New J. Chem.* **2004**, *28*, 1268.

[11] K. C. Kumara Swamy, C. G. Schmid, R. O. Day, R. R. Holmes, *J. Am. Chem. Soc.* **1990**, *112*, 223.

[12] a) V. Chandrasekhar, V. Baskar, R. Boomishankar, K. Gopal, S. Zacchini, J. F. Bickley, A. Steiner, *Organometallics* **2003**, *22*, 3710; b) V. Chandrasekhar, V. Baskar, A. Steiner, S. Zacchini, *Organometallics* **2004**, *23*, 1390.

[13] a) K. C. Kumara Swamy, M. A. Said, S. Nagabrahmanandachari, D. M. Poojary, A. Clearfield, *J. Chem. Soc., Dalton Trans.* **1998**, 1645; b) J. Beckmann, D. Dakternieks, A. Duthie, K. Jurkschat, M. Mehring, C. Mitchell, M. Schuermann, *Eur. J. Inorg. Chem.* **2003**, 4356; c) J. Beckmann, D. Dakternieks, A. Duthie, C. Mitchell, *Organometallics* **2004**, *23*, 6150.

[14] V. Chandrasekhar, V. Baskar, A. Steiner, S. Zacchini, *Organometallics* **2002**, *21*, 4528.

[15] F. Ribot, C. Sanchez, M. Biesemans, F. A. G. Mercier, J. C. Martins, M. Gielen, R. Willem, *Organometallics* **2001**, *20*, 2593.

[16] S.-Y. Song, J.-F. Ma, J. Yang, L.-L. Gao, Z.-M. Su, *Organometallics* **2007**, *26*, 2125.

[17] a) J. Huang, A. Subbiah, D. Pyle, A. Rowland, B. Smith, A. Clearfield, *Chem. Mater.* **2006**, *18*, 5213; b) V. Chandrasekhar, K. Gopal, *Appl. Organomet. Chem.* **2005**, *19*, 429.

[18] a) J. P. Ashmore, T. Chivers, K. A. Kerr, J. H. G. VanRoode, *Inorg. Chem.* **1977**, *16*, 191; b) S. J. Blunden, R. Hill, D. G. Gillies, *J. Organomet. Chem.* **1984**, *270*, 39; c) J. Kowalski, J. Chojnowski, *J. Organomet. Chem.* **1980**, *193*, 191; d) K. C. Molloy, F. A. K. Nasser, J. J. Zuckerman, *Inorg. Chem.* **1982**, *21*, 1711; e) J. Otera, T. Yano, E. Kunimoto, T. Nakata, *Organometallics* **1984**, *3*, 426; f) T. Chivers, J. H. G. vanRoode, J. N. R. Ruddick, J. R. Sams, *Can. J. Chem.* **1973**, *51*, 3702.

[19] R. A. Coxall, S. G. Harris, S. Henderson, S. Parsons, R. A. Taskar, R. E. P. Winpenny, *J. Chem. Soc., Dalton Trans.* **2000**, *14*, 2349.

[20] M. Sathiyendiran, R. Murugavel, *Inorg. Chem.* **2002**, *41*, 6404.

[21] All the hydrogen atoms attached to the phosphate oxygen atoms appeared in the difference map as well resolved peaks. Inclusion of these peaks in successive calculations as hydrogen atoms followed by the refinement of both positional and isotropic thermal parameters resulted in convergence with excellent thermal parameters.

[22] If compound **4** retains the solid-state structure in solution, then three separate ^{31}P NMR resonances with a 2:1:1 intensity distribution should be observed. The actually observed spectrum contains only two resonances of equal intensities with the expected Sn-coupling for the formulation [nBu$_4$Sn$_4$(μ-O)$_2$(tbp-H)$_8$].

[23] JCPDS file no: 35–0028; N. Chernorukov, *Russ. J. Inorg. Chem.* **1979**, *24*, 1294.

[24] JCPDS file no: 75–1143; C.-H. Huang, K. Osvald, A. O. David, D. W. Frank, H. R. Allan, *Can. J. Chem.* **1975**, *53*, 79.

[25] R. Murugavel, M. Sathiyendiran, M. G. Walawalkar, *Inorg. Chem.* **2001**, *40*, 427.

[26] *WinGX, Version 1.64.05*: L. J. Farrugia, *J. Appl. Crystallogr.* **1999**, *32*, 837.

[27] A. Altomare, G. Cascarano, C. Giacovazzo, A. Gualardi, *J. Appl. Crystallogr.* **1993**, *26*, 343.

[28] G. M. Sheldrick, *SHELXL-97, Program for Structure Refinement, University of Göttingen*, Germany, **1997**.

Received: September 24, 2007
Published Online: February 1, 2008

